

# Propagation and interaction of chiral states in quantum gravity

Lee Smolin<sup>\*</sup> and Yidun Wan<sup>†</sup>

Perimeter Institute for Theoretical Physics,  
31 Caroline st. N., Waterloo, Ontario N2L 2Y5, Canada, and  
Department of Physics, University of Waterloo,  
Waterloo, Ontario N2J 2W9, Canada

October 5, 2007

## Abstract

We study the stability, propagation and interactions of braid states in models of quantum gravity in which the states are four-valent spin networks embedded in a topological three manifold and the evolution moves are given by the dual Pachner moves. There are results for both the framed and unframed case. We study simple braids made up of two nodes which share three edges, which are possibly braided and twisted. We find three classes of such braids, those which both interact and propagate, those that only propagate, and the majority that do neither.

---

<sup>\*</sup>Email address: lsmolin@perimeterinstitute.ca

<sup>†</sup>Email address: ywan@perimeterinstitute.ca

# Contents

<b>1</b>	<b>Introduction</b>	<b>3</b>
<b>2</b>	<b>Previous results</b>	<b>5</b>
2.1	Notation . . . . .	6
2.2	Representation of twists . . . . .	6
2.3	Framed and unframed graphs . . . . .	7
2.4	Braids . . . . .	7
2.5	Crossings and chirality . . . . .	7
2.6	Equivalence moves . . . . .	8
2.7	Classification of Braids . . . . .	9
<b>3</b>	<b>Dynamics and evolution moves</b>	<b>10</b>
3.1	The $2 \rightarrow 3$ move . . . . .	12
3.2	The $3 \rightarrow 2$ move. . . . .	13
3.3	The $1 \rightarrow 4$ move . . . . .	13
3.4	The $4 \rightarrow 1$ move . . . . .	14
3.5	The unframed case and the role of internal twist . . . . .	16
3.6	A conserved quantity . . . . .	16
<b>4</b>	<b>Stability of braids under the evolution moves</b>	<b>17</b>
<b>5</b>	<b>Braid Propagation</b>	<b>17</b>
5.1	Examples of chiral propagation . . . . .	20
5.2	Which braids can propagate? . . . . .	21
<b>6</b>	<b>Interactions</b>	<b>22</b>
6.1	Examples of interacting braids . . . . .	27
6.2	General results on interactions . . . . .	28
<b>7</b>	<b>Conclusions</b>	<b>31</b>

# 1 Introduction

There is an old dream that matter is topological excitations of the geometry of spacetime. Recently it was discovered that this is realized in the context of models of quantum geometry based on spin networks, such as those used in loop quantum gravity and spin foam models[1, 2, 3]. Although the rough idea that topological features of spacetime geometry might be interpreted as particles is very old, two questions delayed implementation of the idea till recently. First, how do we identify an independent excitation or degree of freedom in a background independent quantum theory, where the semiclassical approximation is expected to be unreliable? Second, why should such excitations be chiral, as any excitations that give rise to the low mass observed fermions must be?

Recently a new approach to the first question was proposed in [1, 2], which was to apply the notion of noiseless subsystem from quantum information theory to quantum gravity, and use it to characterize an emergent elementary particle. The key point is that noiseless subsystems arise when a splitting of the hilbert space of the whole system (in this case the whole quantum geometry) into system and environment reveals emergent symmetries that can protect subsystems from decohering as a result of inherently noisy interactions with the environment. The proposal raised the question of whether there were models of dynamical quantum geometry in which this procedure reproduced at least some of the symmetries of the observed elementary particles.

This led to an answer to the second question. In [3] it was shown that this was the case in a simple model of the dynamics of quantum geometry. The result of that paper incorporated prior results of [4] where a preon model was coded into a game of braided triplets of ribbons. The needed ribbon graphs are present in models related to loop quantum gravity when the cosmological constant is non-zero[5, 6]; and the three ribbon braids needed are indeed the simplest systems in that model bound by the conservation of topological quantum numbers. Strikingly, the results of [3] make contact with both structures from topological quantum computing and now classic results of knot theory from the 1980s. In both chirality plays a key role because braids are chiral and topological invariants associated with braided ribbons are able to detect chirality and code chiral conservation laws.

Many questions remained unanswered however. One was quickly answered in [7]: can the excitations be considered local in the quantum geometry? The answer is that many of the braided excitations can be evolved by local moves to states which can be considered local because they are attached by only a single edge to the rest of the graph representing the quantum geometry of space. The same paper answered in the affirmative another question: do these excitations propagate? If the quantum geometry of space can be modeled as a large and complicated spin network graph, [7] showed that the braids which code the excitations propagate on the larger graph under the local dynamical moves of the model.

However, the results of [3] suffered from a serious limitation. The conservation laws which preserve the excitations are exact, which means that there can be no creation and

annihilation of particles. Indeed, as shown by [7] the braided excitations of [3] are like solitons in integrable systems: they pass right through each other. This means that interactions necessary to turn the game coded in [3] into a real theory of the standard model do not appear to exist in that model.

As a result, a search has been underway for a modification of the dynamics studied in [3] which would allow propagation and interactions of emergent chiral matter degrees of freedom[8]. This is not so easy as many extensions of the local moves studied in [3] destabilize the braids so that there are no longer any emergent conservation laws.

In this paper we report on one successful such modification. This is based on two ideas proposed by Markopoulou[9]. First extend the graphs in the model from three valent to four valent and base the dynamics on the dual Pachner moves naturally associated with four valent graphs. Second, only allow the dual Pachner moves when acting on a subgraph which is dual to a triangulation of a trivial ball in  $R^3$ .

Four-valent graphs and the corresponding dual Pachner moves naturally occur in spin foam models[10], hence this extends the results on the existence of emergent, chiral degrees of freedom to that much studied case. As we will show below, the dual Pachner moves, with the restriction to duals of triangulations of trivial regions, is exactly right to preserve the stability of certain braid states, while giving some propagation and interactions. We do not however, in this paper, investigate the correspondence to the preon models of [4, 3].

In many studies of spin foam models the graphs and spin foam histories are taken to be abstract, or unembedded. Our results do not directly apply to these models, as the topological structures our results concern arise from the embedding of the graphs in a topological three manifold. But neither do such models give dynamics for states of loop quantum gravity, which are embedded. A path integral formulation of loop quantum gravity must give evolution amplitudes to embedded graphs, as those are the states found by quantizing diffeomorphism invariant gauge theories such as general relativity.

We study here two cases of four valent embedded graphs. The first are framed, which means that the edges are represented by tubes which meet at nodes which are punctured spheres. If we take the limit where the edges become curves, while the nodes remain punctured spheres we get the unframed case.

One might go further and consider the case in which the nodes are structureless points rather than punctured spheres. However, in this case the dual Pachner moves are not all well defined in the embedded case, so that there cannot be an application of spin foam models to amplitudes for such graphs which incorporate dual Pachner moves.

The main results of this paper are as follows:

- The dual Pachner moves on embedded four valent graphs may be restricted to those that are dual to Pachner moves on triangulations of regions of  $\mathbb{R}^3$ , in such a way that some chiral braid states are locally stable, which means they cannot be undone by local moves involving the nodes that comprise them.

- Some of those stable chiral braids propagate, in the sense that under the local evolution moves they can exchange places with substructures adjacent to them in the graph. The propagation in most cases is chiral. In these cases a braid will propagate along an edge in the larger graph only to the left and its mirror image (which is a distinct state) will propagate only to the right.
- Results are found which limit the classes of propagating states.
- In some cases two braids adjacent to each other in a spin network may merge under the action of the local moves. For this to happen one of them must be in a small class of states called actively interacting. We find examples of actively interacting braids, all of which are equivalent to trivial braids with twists.

This is the second of a series of papers in which the conservation, propagation and interactions of four valent spin networks are investigated. The first paper [11] contains results on classifications of the relevant braid embeddings and it also establishes our notation. For completeness we give a summary of the notation and main results of that paper in the next section. The dynamics is then introduced in section 3, by giving the allowed set of dual Pachner moves by which embedded graphs are allowed to evolve. In section 4 we discuss the local stability of the braids under the equivalence and evolution moves and introduce a quantity that is conserved under both. Section 5 gives examples of braids propagating as well as some results which limit which braids can propagate. Section 7 does the same with interactions.

## 2 Previous results

We work with a graphic calculus which describes 4-valent framed spin-networks embedded in 3-manifolds up to diffeomorphisms. The graphs represent the networks and their embeddings in terms of two dimensional diagrams which represent projections of the graphs onto a two-plane. As the spin or, more generally, representation, representation labels play no role in the results of this paper, they are not indicated in these diagrams. The notation we use was described in detail in [11], in this section we review the notation and the results we will need from that paper.

When using this notation it is important to keep in mind the distinction between braids, which are diffeomorphism equivalence classes of embeddings of diagrams in three dimensional space, and the braid diagrams that represent them. Many braid diagrams will correspond to the same braid, these will be related by a set of equivalence moves. It will be important also to distinguish these equivalence moves from dynamical moves we introduce in the next section, which take equivalence classes, or braids, to equivalence classes.

## 2.1 Notation

In the category of framed graphs we discuss edges that are represented by tubes and nodes that are represented by 2-spheres with the incident edges attached at circles called punctures. We consider only four valent nodes which are non-degenerate so that not more than two edges of a node are co-planar. Since we are interested in projections representing graphs up to diffeomorphisms, there is a single diffeomorphism class of nodes. For convenience, the nodes are all represented as rigid and dual to tetrahedra, as shown in Fig. 1. We will limit ourselves to projections in which all nodes are in one of the configurations or states shown in Fig. 1. Because of the freedom to make a diffeomorphism before projecting this can be done without loss of generality. We note that as shown in Fig. 1 the different such allowed projections are related to each other by rotations of  $\pi/3$  around an axis defined by one of the edges.

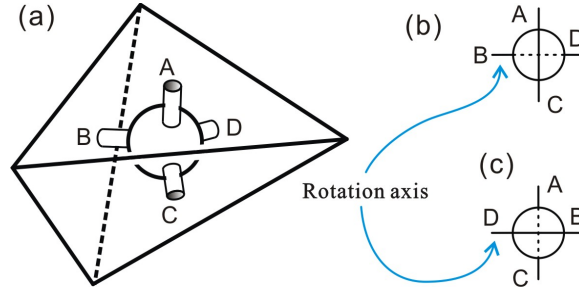


Figure 1: (a) is a tetrahedron and its dual node. There are two orientations of a node that can appear in a diagram (b) denotes the  $\oplus$  state, while (c) denotes the  $\ominus$  state.

## 2.2 Representation of twists

As we have noted, the possible states by which a node may be represented in a projection can be taken into each other by  $\pi/3$  rotations around one of the edges. By the local duality of nodes to tetrahedra, these correspond to the  $\pi/3$  rotations that relate the different ways that two tetrahedra may be glued together on a triangular face. These rotations cause twists in the edges and, as a result of the restriction on projections of nodes we impose, the twists in a projection of an edge of a graph will be in units of  $\pi/3$ . This allows a simple representation of twists of edges which is shown in Fig. 2(a).

We note that the twist indicated in 2(a) is equivalent to that shown in 2(b). This provides a way simplifying the notation, as it allows us to label an edge with a right-handed twist by a positive integer (and left-handed twist by a negative integer). Thus, Fig. 2(a) and (b) can be replaced by 2(c) without introducing any ambiguity.

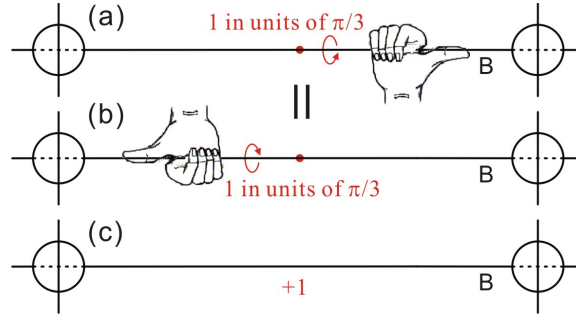


Figure 2: The 1 unit of twist (equivalent to a  $\pi/3$  rotation) in (a) means cut to the right of the red dot and twist as shown. This is equivalent to the opposite twist on the opposite side of the red dot, as shown in (b). Thus, both may be represented as in (c), by a label of +1 of edge  $B$ .

### 2.3 Framed and unframed graphs

Most of the results of this paper will refer to the case of framed graphs, defined above. However, unframed graphs are used in loop quantum gravity and it is useful to have results then for that case as well. To do that we need a particular definition of unframed graphs, which is gotten from the framed case discussed here by dropping information about rotations or twists of the edges, but keeping the nodes as spheres, locally dual to tetrahedra. This is necessary so that the dual Pachner moves are well defined for embedded graphs. If we drop the resolution of nodes as spheres, and represent them as structureless points which are just intersections of edges, we lose the information as to which pairs of edges at a node are over or under (in the sense of Fig. 1) and the dual Pachner moves which will be defined in the next section will no longer be well defined.

In the rest of this paper we refer always to the framed case, unless we explicitly describe results for the unframed case.

### 2.4 Braids

We will be interested in a class of embedded sub-spinnets which consist of two nodes which share three edges which may be braided. These are defined as braids, whose two dimensional projections are called braid diagrams[11]. An example of such a braid diagram is shown in Fig. 3. In the rest of the paper, we use braids for both braids and their braid diagrams, unless an emphasis on braid diagrams is necessary.

### 2.5 Crossings and chirality

As usual we can assign a number to a crossing according to its chirality, viz +1 for a right-handed crossing, -1 for a left-handed crossing, and 0 otherwise. Fig. 4 shows this

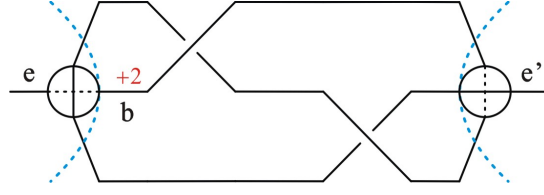


Figure 3: A typical 3-strand braid diagram formed by the three common edges of two end-nodes. The region between the two dashed line satisfies the definition of an ordinary braid. Edges  $e$  and  $e'$  are called external edges. There is also a right handed twist of 2 units on strand  $b$ . In this figure the left handed node is in an  $\oplus$  state while the right handed node is in an  $\ominus$  state.

assignment.

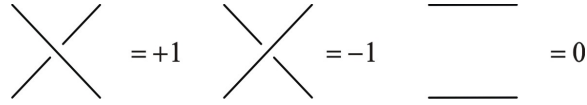


Figure 4: The assignments of right-handed crossing, left-handed crossing, and null crossing respectively from left to right.

## 2.6 Equivalence moves

Diffeomorphism classes of embedded knots and links are described in terms of two dimensional diagrams which represent projections of the embedded graphs onto a two dimensional plane. Many projections, hence many diagrams, represent the same diffeomorphism equivalence class of an embedded graph. In the case of knots and links without nodes this is reflected in Reidemeister's theorem which gives a small number of local moves in the diagrams such that any two diagrams represent the same three dimensional diffeomorphism equivalence class iff they are related by a finite sequence of such moves.

For the class of framed four valent graphs with rigid nodes, the Reidemeister moves are extended by two classes of moves[11].

- Translations in which nodes are slid over or under crossings in the diagram, as shown in Figures 5 and 6.
- Rotations, which are exhibited in Figures 7 and 8 generate equivalences between diagrams as shown in Fig. 9.



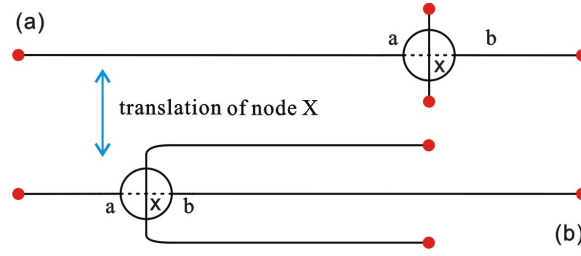


Figure 5: Red points I and J represent other nodes where edges  $a$  and  $b$  are attached to. (b) is obtained from (a) by translating node  $X$  from right to left, and vice versa.

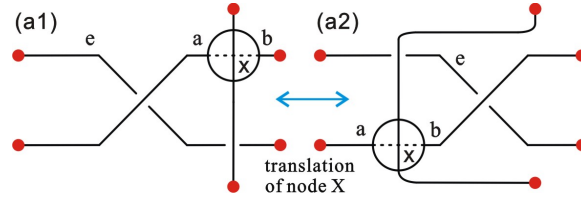


Figure 6: Red points represent other nodes where edges  $a$  and  $b$  are attached to. (a1) and (a2) can be transformed into each other by translating node  $X$ .

## 2.7 Classification of Braids

A braid diagrams can be equivalent under the equivalence moves to a diagram with a different number of crossings. It is often useful to work with a representative of an equivalence class which has the fewest number of crossings, this motivates the following definition of irreducible and reducible braids:

A braid diagram is **reducible** if it is equivalent to a braid diagram with a fewer number of crossings; otherwise, it is **irreducible**.

The braid on top part of Fig. 9 is an example of a reducible braid, while the bottom of the figure shows an irreducible braid.

It is convenient to talk about end-nodes of braids, which are a portion of a braid including one of the two end nodes. An  $N$ -crossing end-node is said to be a **reducible end-node**, if it is equivalent to an  $M$ -crossing end-node with  $M < N$ , by equivalence moves done on its node; otherwise, it is irreducible.

A braid is **reducible** if it has a reducible end-node. If a braid has a reducible left end-node it is called **left-reducible**. If it has both a left and a right reducible end node it is **two-way-reducible**.

If a braid  $B$  can be reduced to an unbraided, i.e. a braid with no crossing,  $B$  is said to be **completely reducible**.

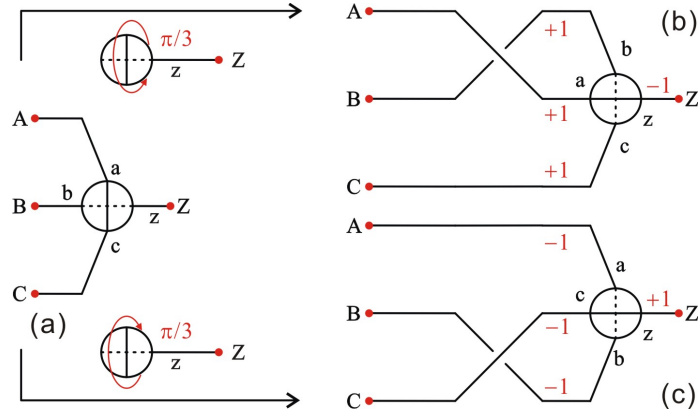


Figure 7: (b) & (c) are results of (a) by rotating the  $\oplus$ -node in (a) w.r.t. edge  $z$  in two directions respectively. Points  $A$ ,  $B$ ,  $C$ , and  $Z$  are assumed to be connected somewhere else and are kept fixed during the rotation. All edges of the node gain the same amount of twist after rotation. Note that a  $\pi$ -rotation changes the state of a node, i.e. if a node is in state  $\oplus$  before the rotation, it becomes a  $\ominus$ -node after the rotation.

The following theorem[11] states that there is no need to investigate end-nodes with more crossings to see if they are irreducible.

**Theorem 1.** *An  $N$ -crossing end-node,  $N > 2$ , which has an irreducible 2-crossing sub end-node, is irreducible.*

### 3 Dynamics and evolution moves

To define the models our results apply to we have to choose a set of dynamical evolution moves. In spin-foams and other models of dynamics of spin networks it is common to pick the dual Pachner moves[10]. To motivate the form of them we posit here it is useful to recall how the Pachner moves arise in combinatorial topology. One defines the topology of a three manifold through operations on a simplicial triangulation. Many different simplicial complexes correspond to the same topological three manifold. Given two of simplicial complexes one wants to know whether they correspond to the same topological three manifold. Pachner's theorem gives the answer, it says they do if the two simplicial complexes can be connected by a finite sequence of local moves, which are called the Pachner moves. They are illustrated in Figures 10 and 14(a).

The dual to a simplicial complex is a framed four valent graph in which nodes are dual to tetrahedra and framed edges are dual to faces. One needs the framing of the graphs to preserve orientations. An edge between two nodes tells us that two tetrahedra, dual to

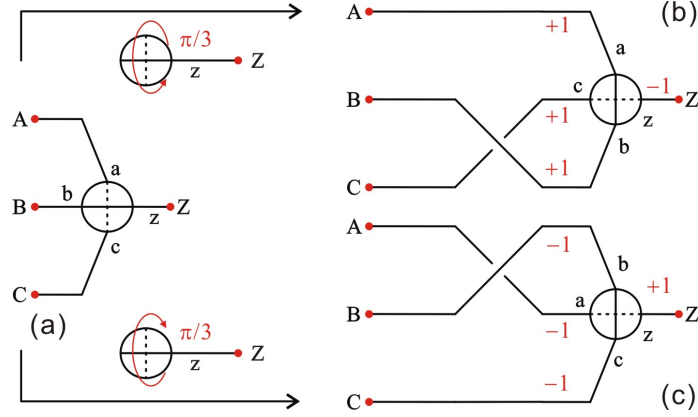


Figure 8: (b) & (c) are results of (a) by rotating the  $\ominus$ -node in (a) w.r.t. edge  $z$  in two directions respectively. Points  $A$ ,  $B$ ,  $C$ , and  $Z$  are assumed to be connected somewhere else and are kept fixed during the rotation. All edges of the node gain the same amount of twist after rotation.

those two nodes, share a triangular face. The framing is needed to tell us how to identify the two triangles.

Let us fix a non-singular differentiable manifold  $\mathcal{M}$  and choose a triangulation of it in terms of tetrahedra embedded in  $\mathcal{M}$  whose union is  $\mathcal{M}$ . Any such simplicial triangulation of  $\mathcal{M}$  has a natural dual which is a framed four valent graph embedded in that manifold,  $\mathcal{M}$ . If one makes a Pachner move on the triangulation, that results in a local move in the framed graph. These are the dual Pachner moves.

However, not every embedding of a framed four valent graph in  $\mathcal{M}$  is dual to a triangulation of  $\mathcal{M}$ . Examples of obstructions to finding the dual include the case of two nodes which share three edges, which are braided, such as shown in Figure 3. This is an embedding of a graph that could not have arisen from taking the dual of a regular simplicial triangulation of  $\mathcal{M}$ . We note that these obstructions are local, in the sense that a subgraph of the embedded graph could be cut out and replaced by another subgraph that would allow the duality to a triangulation of  $\mathcal{M}$ .

This leads to a problem, which is how one defines the dual Pachner moves on subgraphs of embedded graphs which are not dual to any triangulation of  $\mathcal{M}$ . The answer we take is that we do not. This leads to the basic rule:

*Basic rule:* The evolution rules on embedded framed four valent graphs are the dual Pachner moves and they are allowed only on subgraphs which are dual to a ball in  $R^3$ .

We now discuss in detail the allowed moves.

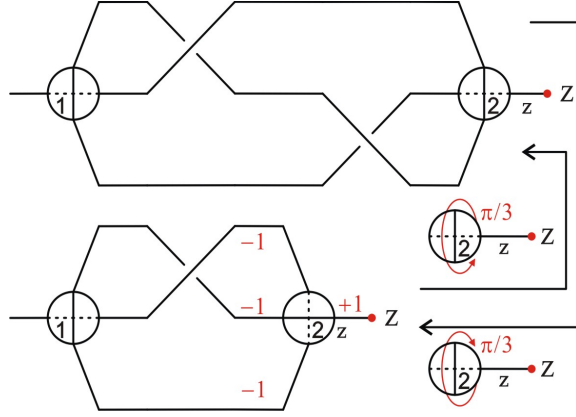


Figure 9: The two braid diagrams are equivalent because they can be transformed into each other by a  $\pi/3$ -rotation of node 2.

### 3.1 The $2 \rightarrow 3$ move

In Fig. 10 we depict the  $2 \leftrightarrow 3$  Pachner move on tetrahedra and the dual move on four valent graphs. One can see that as the result of the move, the 2 vertices together with the edge between them in (a) are replaced by three new vertices and three new edges between them in (b), and vice versa.

The result of a  $2 \rightarrow 3$  move on tetrahedra is unique up to equivalence moves (e.g. rotations). As a consequence the dual  $2 \rightarrow 3$  move on framed graph embeddings is unique.

We next have to translate the allowed  $2 \rightarrow 3$  dual move to the diagrammatic notation introduced in [11] and reviewed in the last section. This is done in Figures 11 and 12.

According to the basic rule, a  $2 \rightarrow 3$  move is only doable on two neighboring nodes with one or more common edges in the case that that subgraph is dual to a triangulation of a ball in  $R^3$ . In terms of our diagrammatic notation this translates into the following conditions.

**Condition 1.** A  $2 \rightarrow 3$  move is doable on two nodes if and only if

1. the two nodes have one and only one common edge and can be arranged in either of the forms in Fig. 11(a) or Fig. 12(a);
2. there is no twist (in the framed case) on the common edge (note that if there is a twist on the common edge, one has to rotate either of the node to annihilate the twist);
3. the states of the two nodes with respect to the common edge are either both  $\oplus$  or both  $\ominus$ .

The reasoning for the above conditions are easily understood in terms of the local dual picture of tetrahedron. If Condition 1 holds for two neighboring nodes, there will be no twist on the edges forming the loop generated by the  $2 \rightarrow 3$  move, as shown in above figures.

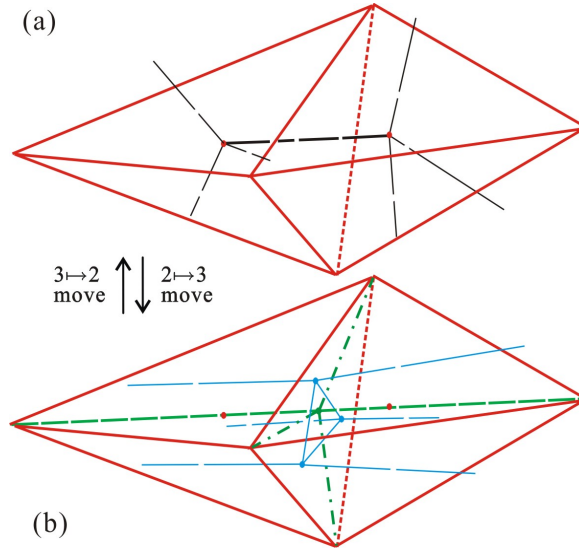


Figure 10: (a) shows two tetrahedra with a common face; the black lines represent the dual graph. (b) shows the three tetrahedra which result from a  $2 \rightarrow 3$  Pachner move applied to the pair of tetrahedra in (a); the blue lines indicate the dual graph.

### 3.2 The $3 \rightarrow 2$ move.

The  $3 \rightarrow 2$  Pachner move is the inverse of the  $2 \rightarrow 3$  Pachner move. It requires three tetrahedra each pair of which share a face. By taking the dual one finds a  $3 \rightarrow 2$  move on embedded framed four valent graphs, it operates on three nodes that are connected in pairs to make a triangle. The basic rule imposes conditions of a legal  $3 \rightarrow 2$  move which are as follows.

**Condition 2.** A  $3 \rightarrow 2$  move is doable on three neighboring nodes if and only if

1. the three nodes with their edges can be arranged in one of the four proper configurations, namely Fig. 11(b), (c) and Fig. 12(b), (c);
2. the loop formed by common edges of the three nodes is contractible, i.e. there is no other edges going through the loop or tangled with the loop. See Figures. 13(a) & (b);
3. In the framed case there should be no twist on the edges forming the loop (such twists are henceforth called **internal twists**); Fig. 13(c) shows a counter-example.

### 3.3 The $1 \rightarrow 4$ move

The  $1 \rightarrow 4$  Pachner move is a decomposition of a single tetrahedron into four tetrahedra contained in it. Its dual is a move that takes a node and replaces it by four nodes, connected together as a tetrahedra. This is illustrated in Fig. 14.



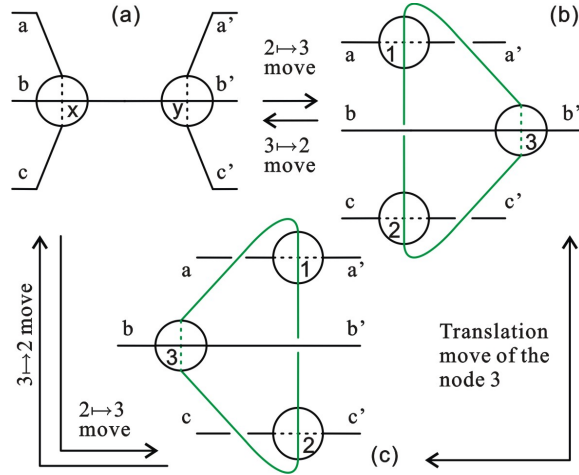


Figure 12: (a) is the original configuration of two nodes in  $\ominus$ -state, ready for a  $2 \rightarrow 3$  move. (b) is a result of the  $2 \rightarrow 3$  move from (a); it also leads to (a) via a  $3 \rightarrow 2$  move.

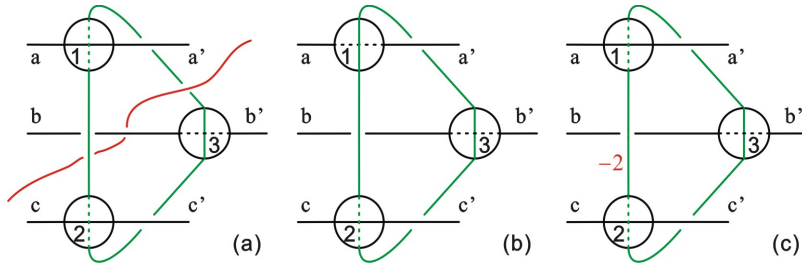


Figure 13: (a) & (b) are not configurations for a legal  $3 \rightarrow 2$  move due to respectively the red edge and edge  $a'$  going throught the green loops, which makes the latter incontractible; (c) is not either because of the  $2\pi/3$ -twist on a green edge.

which are as follows.

**Condition 3.** A  $4 \rightarrow 1$  move is doable on four nieghboring nodes if and only if

1. the four nodes together with their common edges can be arranged as shown in Fig. 14(c) or its parity inverse;
2. the loops are all contractible i.e. there is no any other edge going through the loop or tangled with the loop; (See Fig. 13 for a similar situation.)
3. there should be no internal twists on closed loops in the initial diagram.

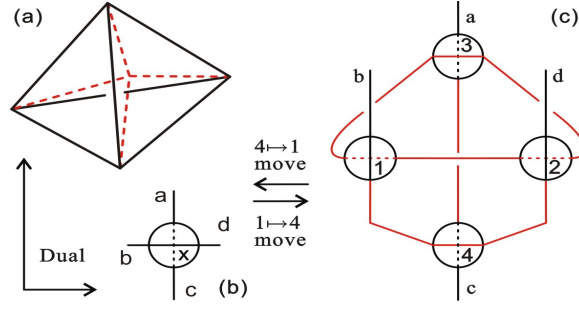


Figure 14: (a) shows how a  $1 \rightarrow 4$  move is viewed with tetrahedra; dashed red lines illustrate the splitting of the big tetrahedron into four tetrahedra. (b) is the node dual to the big tetrahedron in (a). (c) is obtained from (b) by a  $1 \rightarrow 4$  move, which can go back to (b) by a  $4 \rightarrow 1$  move. Red lines in (c) are the edges generated by the move.

### 3.5 The unframed case and the role of internal twist

The same evolution moves apply in the unframed case, since the structure in the nodes is sufficient to define the dual Pachner moves. One can also posit an extension of the class of theories just described in which internal twist is allowed on closed loops that are annihilated by the  $3 \rightarrow 2$  move or  $4 \rightarrow 1$  move. We will see below examples in which this enlarges the class of propagating braids.

### 3.6 A conserved quantity

Rotations create or annihilate twist and crossings simultaneously. As a result, in the framed case, a certain combination of them is an invariant, which we call the **effective twist number**[11]. Given a connected subdiagram,  $\mathcal{R}$ , and an arbitrary choice of orientations on the edges of  $\mathcal{R}$ , this is defined by,

$$\Theta_0 = \sum_{\text{all edges in } \mathcal{R}} T_e - 2 \times \sum_{\text{all Xings in } \mathcal{R}} X_i, \quad (1)$$

where  $T_e$  is the twist number created by the rotation on an edge of the sub-diagram,  $X_i$  is the crossing number of a crossing created by the rotation between any two edges in the sub-diagram, and the factor of 2 comes from the fact that a crossing always involve two edges. One can easily check that the rotations and translations just defined, carried out within  $\mathcal{R}$ , preserve  $\Theta_0$ .

$\Theta_0$  extends to a quantity which is conserved also under the evolution moves, with the following modifications. Within a subdiagram  $\mathcal{R}$ , the edges and nodes of the diagrams define continuous curves where the edges continue across the diagrams as noted (that is each node projection gives a choice of the four incident edges into two pairs, each of which is connected through the node.) These curves are of two kinds, open which end at



two points on the boundary of  $\mathcal{R}$  and closed. In addition, define an *isolated substructure*[7] to be a subgraph which is attached to the rest of the graph by a single edge.

- Choose an arbitrary orientation of the open curves.
- Sum over the orientations of the closed curves.
- In the countings of crossings all crossings of edges with edges in isolated substructures are to be ignored.

Then the following is conserved under all equivalence moves and evolution moves that act entirely within  $\mathcal{R}$ .

$$\Theta_{\mathcal{R}} = \sum_{\text{Orientations of closed curves in } \mathcal{R}} \left[ \sum_{\text{all edges in } \mathcal{R}} T_e - 2 \times \sum_{\text{all Xings in } \mathcal{R}} X_i \right] \quad (2)$$

## 4 Stability of braids under the evolution moves

Consider a braid of the form of Figure 3. It is not difficult to show that the subgraph formed by the two nodes and the three shared edges is not dual to any triangulation of a ball in  $\mathbb{R}^3$ . Hence a  $2 \rightarrow 3$  move cannot be done on these two nodes. Nor can a  $3 \rightarrow 2$  move be done on any three nodes that contain this pair, for the same reason. Thus, the braid is stable under single moves.

We can extend this to the general observation that any braid whose graph is not dual to a triangulation of a ball in  $\mathbb{R}^3$  is stable under single allowed moves. We believe that there is a stronger stability result for such braids, but postpone consideration of this problem to future work.

## 5 Braid Propagation

We now come to the results on propagation of braids that follow from the evolution moves we have defined here. Because a braids can be considered an insertion in an edge, it makes sense to speak of them propagating to the left or to the right along that edge. To help visualize this in the diagrams we will always arrange a braid so that the edge of the graph it interrupts runs horizontally on the page.

An important note must be made before we get into the details of braid propagation. Recall that braid diagrams correspond to the same diffeomorphism equivalence class if they are connected by a sequence of equivalence moves. It is useful to pick out of each such equivalence class a representative and we do so by requiring that the braid diagram be joined to the larger graph by external edges that are twist free; such a representative

is unique for each equivalence class of braids. This is motivated by the fact that the dynamical moves that we will shortly see initiate propagation and interactions require the external edges by which a braid connects to the rest of the diagram are twist free. The statements that follow concerning propagation and interaction refer to diagrams that satisfy this external edge twist free condition.

We will see that the propagation is in some instances chiral, so some braids propagate only to the left (right), while their mirror images propagate only to the right (left).

We study here a very simple example of propagation, which is the following. A braid is inserted in an edge of a graph as in Fig. 15. We see that there is a node to the right of the braid, with two structures growing out of it. By a series of local moves, the braid moves so that these structures are now attached to a node to the left of the braid, while the braid remains unchanged.

In more detail, a **right-propagation** of a braid  $B$  involves its changing places through a series of evolution moves with a structure  $A$  on its right, which is composed of two sub-spinnet  $S$  and  $S'$  connected by a node  $Y$ , as shown in Fig. 15. The right end-node  $X$  of the braid and node  $Y$  have one and only one common edge.

Begin with an initial condition as shown in Fig. 15(a).

1. Make a  $2 \rightarrow 3$  move on nodes  $X$  and  $Y$  if the move is legal (See Condition 1. The result is shown in Fig. 15(b).
2. Translate nodes 2 and 3 together with their common edge  $g$  to the left, passing all crossings. This may not be possible because a tangle between edge  $g$  and any of the edges  $a$ ,  $b$ , and  $c$  occur (see Fig. 16).
3. Re-arrange nodes 1, 2, and 3 and their edges, by equivalence moves (e.g. rotations), into a proper configuration ready for a  $3 \rightarrow 2$  move (see Condition 2).
4. Do the  $3 \rightarrow 2$  move on nodes 1, 2, and 3; leading to Fig. 15(c), in which the braid  $B$  and the structure  $A$  are both recovered but the braid  $B$  is now on the right of structure  $A$ .

A braid that can propagate to its right is said to be **right-propagating**.

Note that in Fig. 15(a), there is a dashed red line connecting  $S$  and  $S'$ . This means that  $S$  and  $S'$  may possibly be directly connected or connected through another part of the whole spinnet. However, if  $S$  and  $S'$  are indeed so connected there are instances in which the propagation of the braid cannot go through due to the tangle between edges  $s$ ,  $s'$  and the edges of the braid. Thus, if not explicitly stated, the sub-spinnets  $S$  and  $S'$  in the structure  $A$  are assumed to be only connected via the node  $Y$ .

A **left-propagation** is defined similarly in that the unknown structure in a dashed blue square in Fig. (a) is initially on the left of the braid. A braid that can propagate to its left is then called **left-propagatable**. A braid that can propagate to both sides is a **two-way-propagatable** braid.

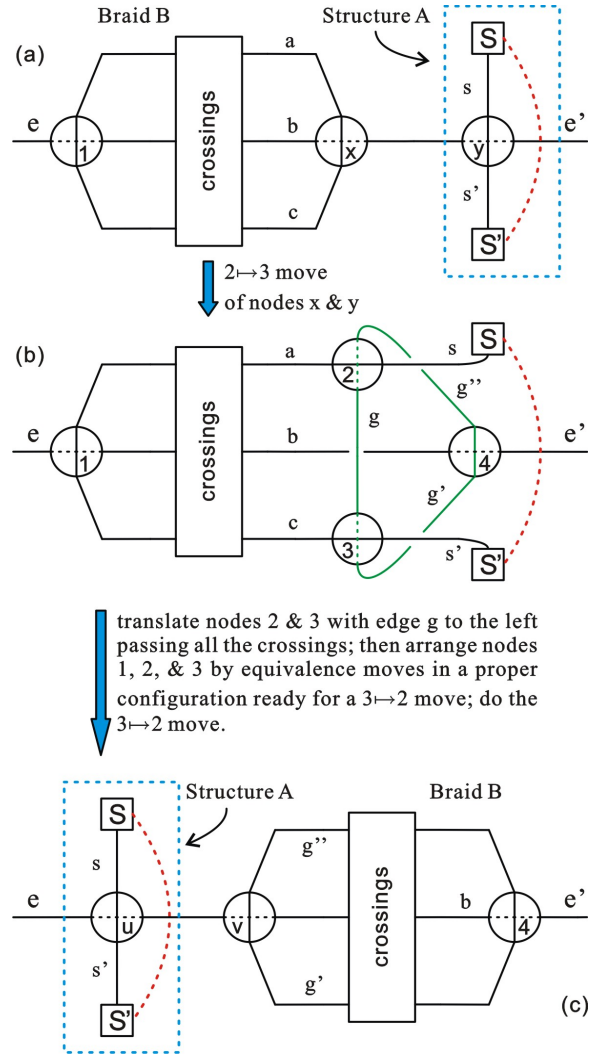


Figure 15: This figure illustrates the process of a right-propagation. (a) shows a braid  $B$  sitting on the left of some arbitrary structure  $A$ , composed of two sub-spinnets  $S$  &  $S'$  connected via a node  $Y$ ; the right end-node of  $B$ , node  $X$ , and node  $Y$  has a common edge; the dashed red line means  $S$  and  $S'$  may or may not be connected via another edge. (b) is obtained from (a) by the  $2 \rightarrow 3$  move on nodes  $X$  and  $Y$ . (c) is the result of the propagation, in which the braid  $B$  and the structure  $A$  are both recovered and exchanged their relative positions, such that  $B$  is now on the right of  $A$ .

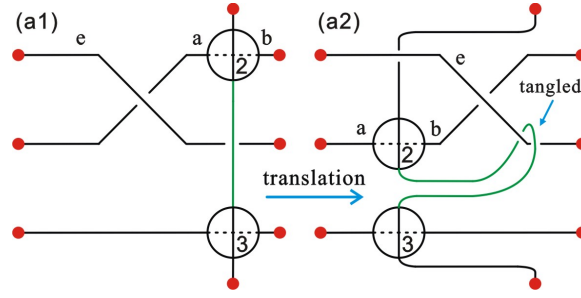


Figure 16: (a2) is obtained from (a1) by translating nodes 2, 3, and their common edge to the left, passing the crossing. A tangle occurs between the edge  $e$  and the common edge of nodes 2 and 3.

## 5.1 Examples of chiral propagation

We now give several examples of right-propagation.

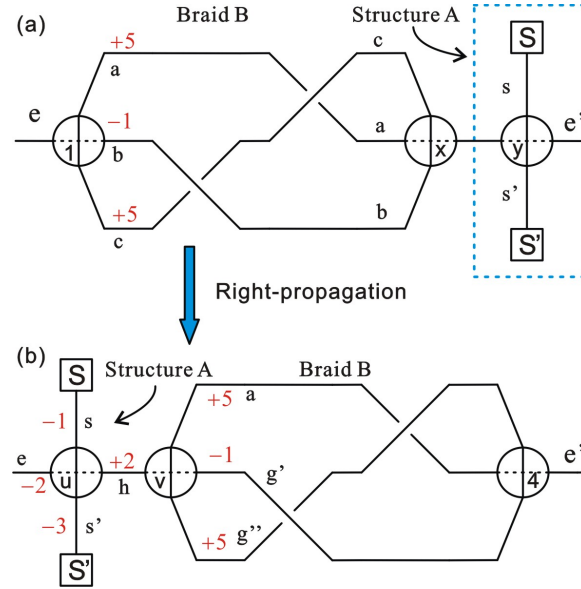


Figure 17: A first example of braid propagation

Our first example is illustrated in Fig. 17. The evolution and equivalence moves required for the propagation of shown in Fig. 17 are given in Fig. 20 for the framed case. For the unframed case they are given in Fig. 21. The braid  $B$  in Fig. 17 propagates only to the right (the reason will be explained by Theorem 2 below).

In fact, it is equivalent to an irreducible 1-crossing braid by a rotation on its right end-node, as drawn in Fig. 18.

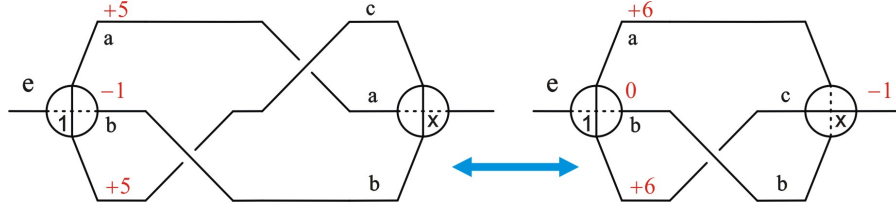


Figure 18: The equivalence between braid  $B$  in Fig. 17, shown on the left, and an irreducible 1-crossing braid, shown on the right.

In the framed case Fig. 17 is one of the examples in which internal twists are present, details of which are illustrated in Fig. 20(g). Hence the braid  $B$  in Fig. 17(a) will not propagate in the framed case unless such moves are allowed. If we do allow the operation of the  $3 \rightarrow 2$  move in this situation, which leads to Fig. 20(h), the propagation succeeds and the initial twists of braid  $B$  are preserved individually, as shown in Fig. 17. In the unframed case, such issues do not arise so the braid is propagating.

A second example of right propagation is given in Fig. 19. This braid is in fact two-way propagating, as can be easily checked. In this example, there is no violation of Condition 2 due to nonzero internal twists. Nevertheless, the initial twists of the propagating braid are not individually preserved under the propagation.

## 5.2 Which braids can propagate?

In fact most braid diagrams propagate neither to the left nor to the right, because of the following result.

**Theorem 2.** *A braid diagram, which is right-irreducible, in a representation in which both external edges are untwisted, does not propagate to the right.*

*Proof.* We prove this for the case of right-propagation; the left one follows similarly. If a braid is not right-reducible, it means that the braid has an irreducible 1-crossing right end-node. The idea is to show that the crossing of each of these irreducible 1-crossing end-nodes causes a tangle during translating the nodes generated by a  $2 \rightarrow 3$  move. There are four irreducible 1-crossing right end-nodes in total, we pick one to demonstrate the proof, which is depicted in Fig. 22. In view of this, the proof for the other three irreducible nodes are straightforward.  $\square$

At first this result may seem puzzling. If a reducible braid diagram  $B$  propagates to the left, why doesn't the irreducible braid diagram  $B'$  it reduces to? Looking at Fig. 18 we see that the point is that an irreducible diagram can propagate, when it, together with its environment, is equivalent to a diagram which has propagation. But in those cases the requirement of having twist free external edges is not met, precisely because the

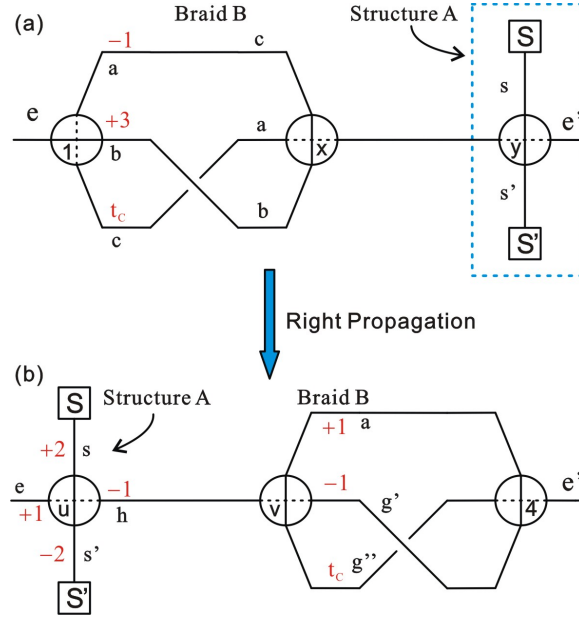


Figure 19: A second example of right propagation. Note that the twist  $t_c$  on strand  $c$  is arbitrary but the total twist is now not conserved.

equivalence move required to take the irreducible diagram to one that does propagate introduces a twist.

This theorem has two immediate corollaries.

**Corollary 1.** *An irreducible braid diagram, in a representation in which both external edges are untwisted, does not propagate either way.*

*Proof.* An irreducible braid is neither left- nor right-reducible; therefore, it does not propagate to either left or right, i.e. it does not propagate.  $\square$

**Corollary 2.** *If a right-reducible braid diagram propagates, in a representation in which both external edges are untwisted, it only propagates to the right. The proof is obvious.*

Examples of left-propagating braids are of course given by the mirror images of the right-propagating braids. If one flips the crossing on the left of braid  $B$  in Fig. 17(a), one obtain an example of two-way propagating braids.

## 6 Interactions

We show now that in a few circumstances braids can interact with each other, in the sense that two braids can meet and turn through a sequence of local moves into a single braid.

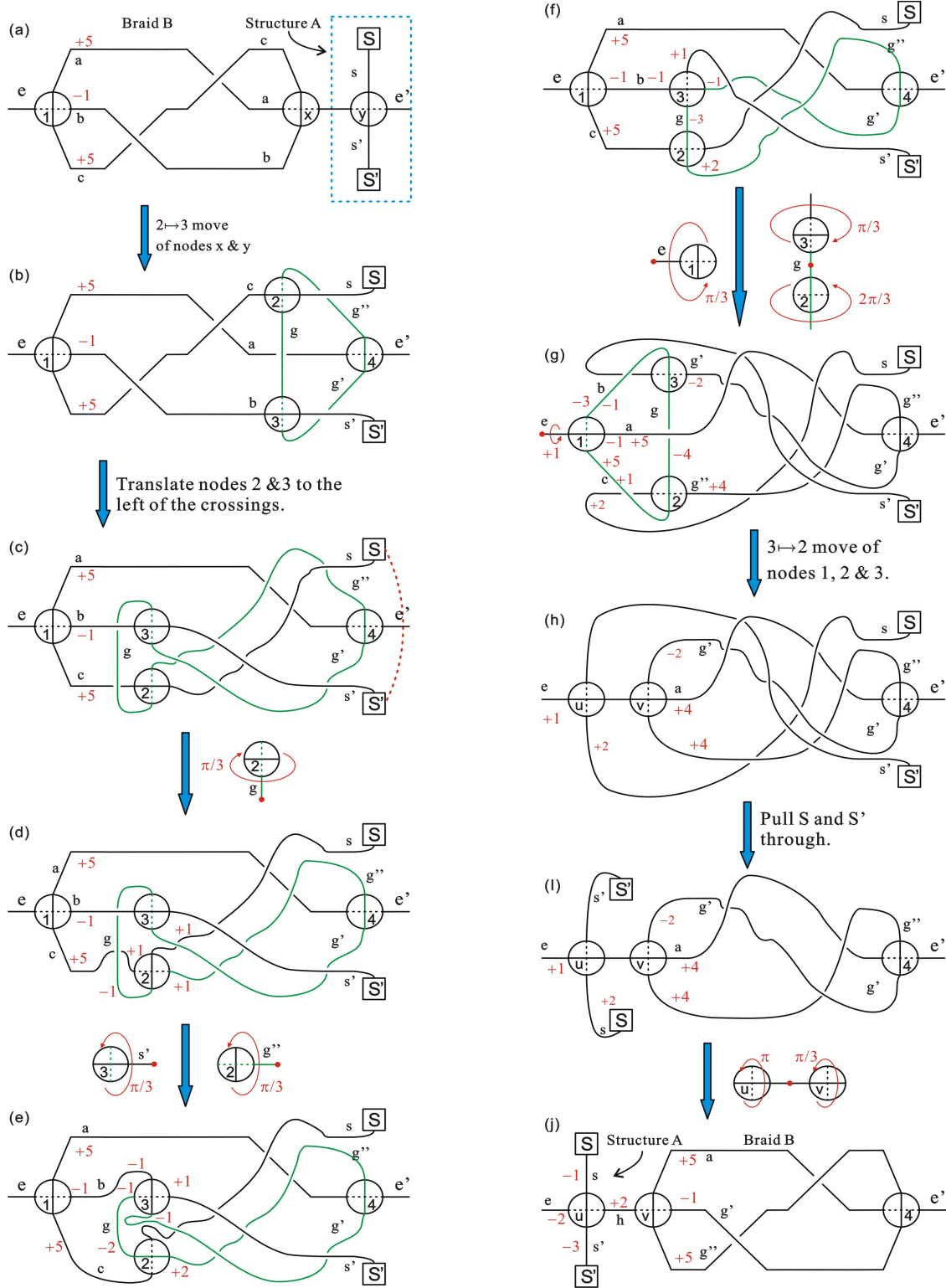


Figure 20: The details of the first example of braid propagation, in the framed case.

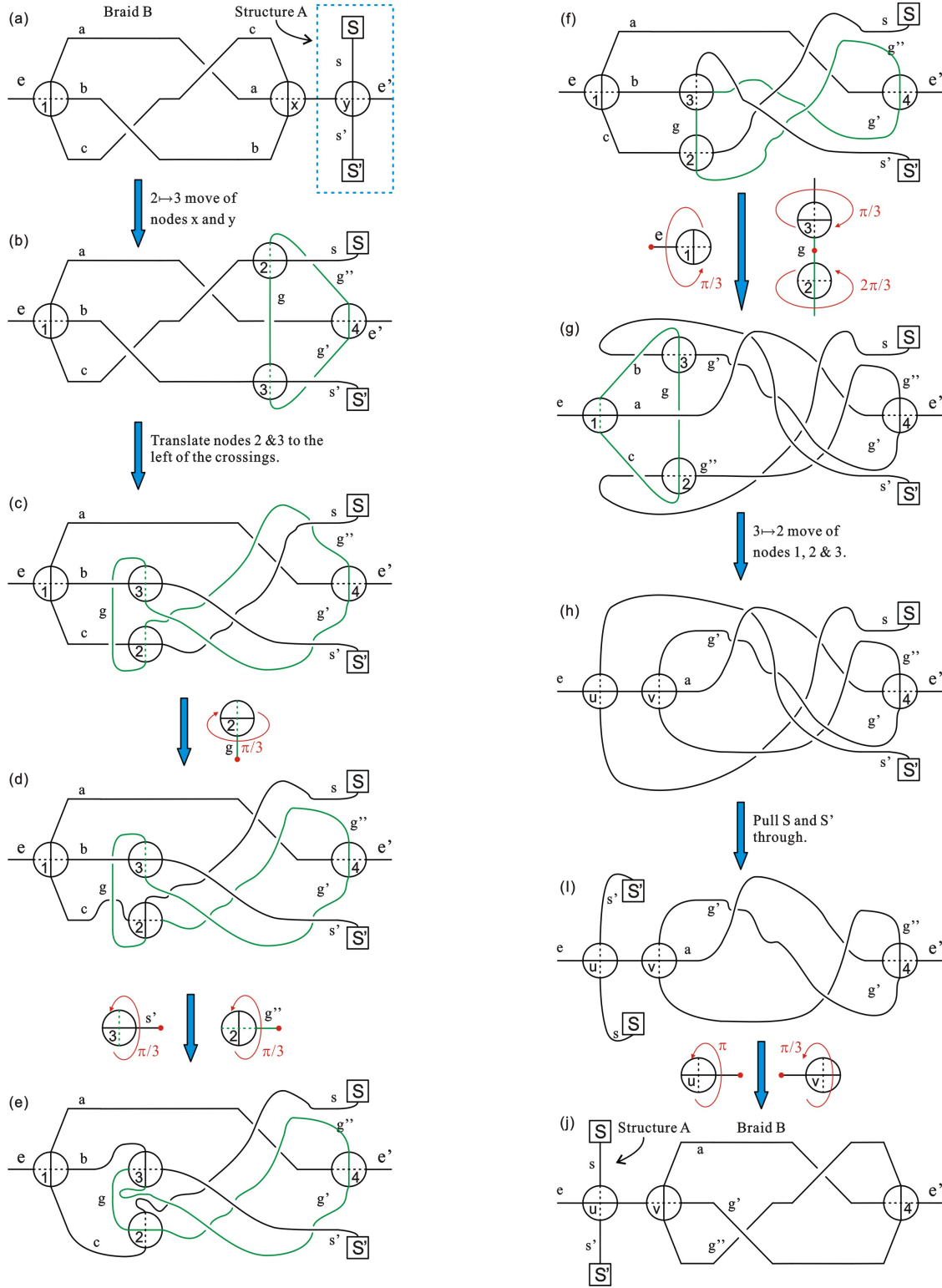


Figure 21: The details of propagation in the unframed case.



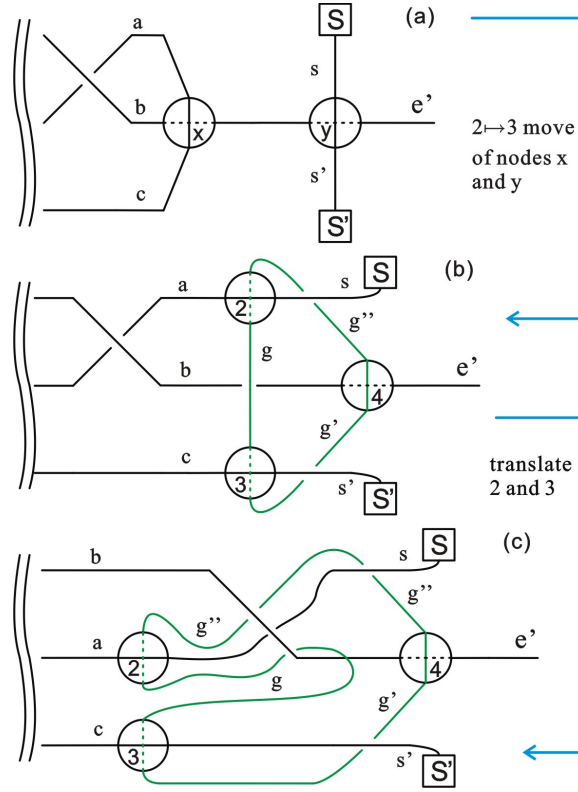


Figure 22: (a) contains an irreducible 1-crossing right end-node, which belongs to a braid whose left side is neglected, and a structure as that in Fig. 15(a). (b) is obtained from (a) by a  $2 \rightarrow 3$  move on nodes  $X$  and  $Y$ . (c) is the result of translating nodes 2, 3 and edge  $g$  to the left, passing the crossing, which causes a tangle between edge  $g$  and edge  $b$ . Note that the crossing between edges  $a$  and  $b$  in Fig. 22(a) turns out to be a crossing between edges  $g''$  and  $b$ ; a similar situation has been seen in Fig. 16.

This will be possible in the case that at least one of the braids are of a special class called *actively interacting*. As the moves are time reversal invariant, it is also possible for a single braid to decay to two braids, so long as one of the products is of this special class.

The initial condition for an interaction has two braids adjacent to each other along an edge. Such a state can be reached by either or both braids propagating along an edge. Then in some cases there is a series of local moves resulting in a single braid. This is illustrated in Figure 23. The time reversed history will then give a case of a single braid decaying to two braids that can then propagate separately.

It turns out that braids may interact actively or passively. If a braid interacts actively, it can interact with any braid it encounters, and hence are called *actively interacting*. All other braids interact only passively, i.e. only if they encounter an actively interacting braid. We will see shortly how and when a braid can be actively interacting. We note also

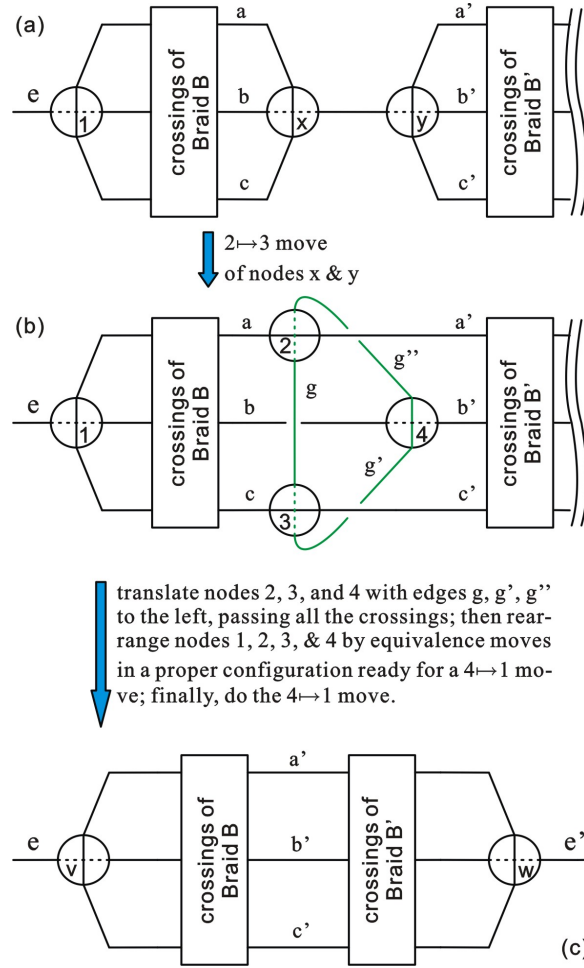


Figure 23: The interaction of two braids.

the possibility that braids may interact from the left or right, so we distinguish those two possibilities.

As in the case of propagation, the **active right-interaction** of a braid  $B$  with a neighboring braid  $B'$  proceeds through a series of steps, indicated in Fig. 23. Each step must be a possible evolution or equivalence move for the interaction to take place.

1. Begin with the initial condition 23(a). As in the case of propagation first make a  $2 \rightarrow 3$  move on nodes  $X$  and  $Y$ , leading to the configuration shown in Fig. 23(b).
2. If possible, without creating any tangles of the kind shown in Fig. 16, translate nodes 2, 3, and 4 together with their common edge  $g, g',$  and  $g''$  to the left, passing all crossings of  $B$ .
3. If possible, re-arrange nodes 1, 2, 3, and 4 with their edges, by equivalence moves

into a configuration which allows  $4 \rightarrow 1$  move.

4. If possible (see Condition 3), do the  $4 \rightarrow 1$  move on nodes 1, 2, 3, and 4, resulting in Fig. 23(c).

The actively interacting braid is the one which the three nodes are pulled through, in this case it is braid  $B$ . We will see shortly that the class of such braids is very limited. The other braid, which may be arbitrary, is said to have passively interacted.

## 6.1 Examples of interacting braids

As we shall see in the next subsection, most braids do not actively interact. Because the last step of an interaction is a  $4 \rightarrow 1$  move, the possibilities are limited because the initial step of a  $4 \rightarrow 1$  move requires four nodes making up a tetrahedron. Here the issue raised above of how restrictive are the rules for a  $4 \rightarrow 1$  move comes in. If we are less restrictive and allow internal twists, we get more actively interacting braids.

Even allowing moves that annihilate internal twists, all the examples we have so far found of actively interacting braids are equivalent to the unbraid, made up of three strands with no crossings, but with twists on the edges.

Our first example of interaction is shown in Fig. 24. Fig. 24(a) depicts two braids: a 1-crossing braid  $B$  on the left of a braid  $B'$  with arbitrary crossings and twists. The right end-node  $W$  of braid  $B'$  is irrelevant, which can be either  $\oplus$  or  $\ominus$ , here we assume it in the state  $\ominus$  for the convenience of showing the left-interaction later. One may notice the  $2\pi/3$ -twist on edge  $c$  of braid  $B$ , the presence of which may be essential for the interaction to be done and will be explained shortly. The active right-interaction of braid  $B$  on  $B'$  results in the new braid shown in Fig. 24(b); one can see that the initial twist of braid  $B$  in Fig. 24(a) is preserved in Fig. 24(b) under the interaction.

The complete steps for the interaction are shown in Fig. 25. In Fig. 25(f), the initial twist on strand  $c$ ,  $-2$ , of braid  $B$  cancels the twist,  $+2$ , created by rotations, such that nodes 1, 2, 3, and 4 with their common edges are in a proper configuration for a  $4 \rightarrow 1$  move, satisfying Condition 3. In addition, surprisingly, as already mentioned, the initial twists of braid  $B$  are preserved.

The same braid can interact to the left as well, as we show in Fig. 26.

Note that the braid  $B$  is completely reducible from either end; if we reduce it by a rotation of its right end-node, we get its equivalent braid, Fig. 27(b), which is a trivial braid with twist numbers on all three strands and the right external edge.

A second example of right interaction is shown in Fig. 28. This braid is also left-interacting, as can be easily checked. And it is also equivalent to an unbraid with twists, from top to bottom the twists are 0, 0,  $+2$ , respectively, and a twist  $-2$  on the right external edge. As for the first example, the initial twists in this example cancel the possible internal twists in the process of interaction, and they are individually conserved.

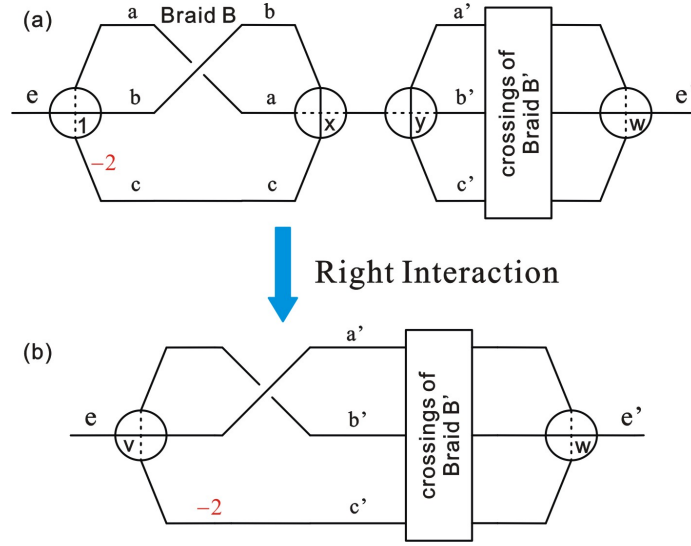


Figure 24: (a) contains a braid  $B$  on the left and a braid  $B'$  with arbitrary crossings & twists on the right. (b) is the resulted braid of the active right-interaction of  $B$  on  $B'$ .

## 6.2 General results on interactions

Now we give some general results which limit the actively interacting braids.

**Corollary 3.** *A (left-) right-irreducible braid is not (left-) actively right-interacting. An irreducible braid is always inactive during an interaction. This also implies that only (left-) right-reducible braids can be actively (left-) right-interacting, which manifests the chirality of interactions.*

*Proof.* This is a corollary of Theorem 2. As shown in Fig. 23, to complete a (left-) right-interaction requires the translation of nodes 2, 3, and 4 together with their common edges  $g$ ,  $g'$ , and  $g''$ . On the other hand, in the proof of Theorem 22 we showed that as long as a braid is (left-) right-irreducible, a tangle between edge  $g$  and original edges of braid  $B$ . Consequently, the translation towards an right-interaction of braid  $B$  will at least cause the tangle between edge  $g$  and strands of the braid, which prevents the final  $4 \rightarrow 1$  move according to Condition 3; hence, the right-interaction cannot be completed as desired. It is the same for a left-interaction. Therefore, if a braid is irreducible, i.e. both left- and right-irreducible, the braid can never actively interact onto another braid; it always behaves inactive in any type of interactions.  $\square$

**Theorem 3.** *If a braid is actively (left-/right-) two-way-interacting, it is also (left-/right-) two-way-propagating.*

*Proof.* The proof contains two parts.

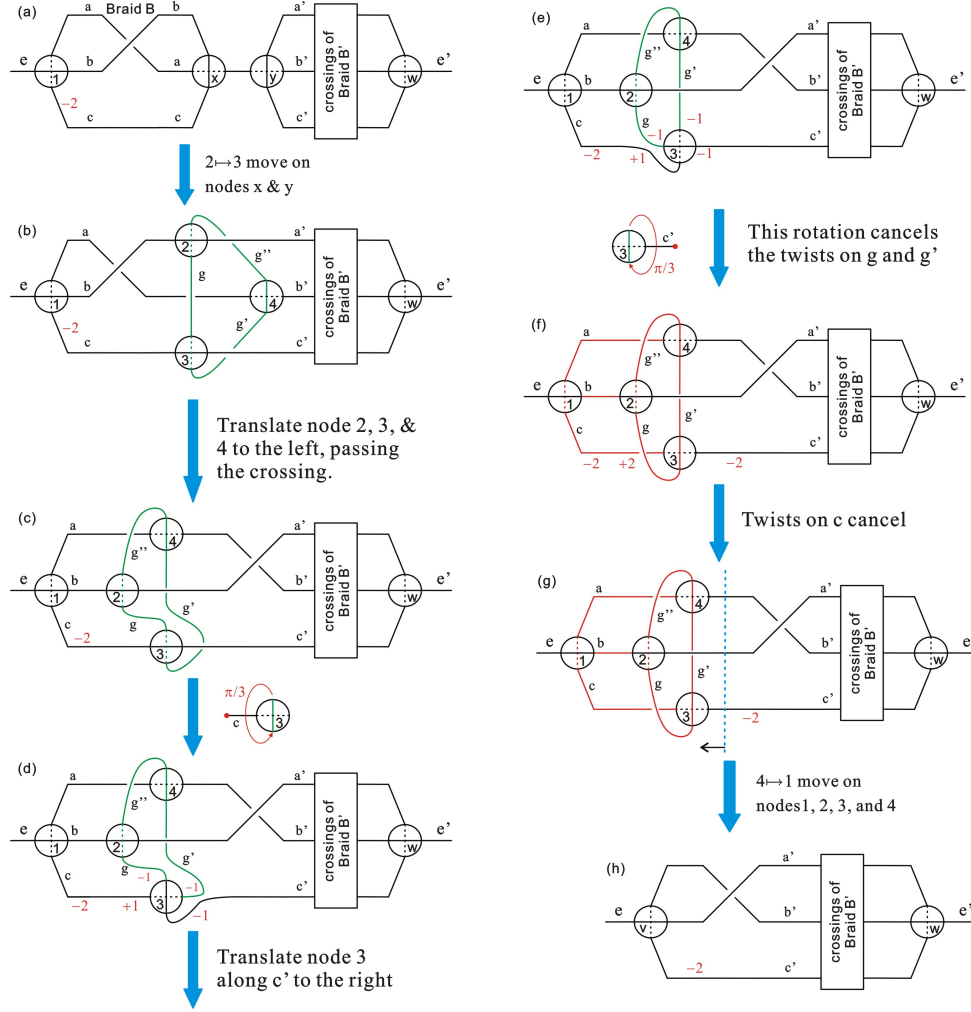


Figure 25: The details of the first example of interacting braids, Fig. 24.

1) We notice that in doing an interaction one needs to translate all the three nodes (say nodes  $\alpha$ ,  $\beta$ , and  $\gamma$ ) and their common edges, obtained from the initial  $2 \rightarrow 3$  move, all the way through the crossings of the active braid, say braid  $B$ . However, if braid  $B$  is to propagate in the same direction, two of the nodes  $\alpha$ ,  $\beta$ , and  $\gamma$  must be successfully translated. Therefore, if braid  $B$  is able to actively interact to the left (right), i.e. the translation of  $\alpha$ ,  $\beta$ , and  $\gamma$  does not cause any tanglement, the translation of any two of the three nodes should not lead to any tanglement either.

2) Given part 1), if braid  $B$  can actively interact, after being translated nodes  $\alpha$ ,  $\beta$ , and  $\gamma$  together with an end-node (say node 1) of braid  $B$  can be arranged in a proper configuration for a  $4 \rightarrow 1$  move. There is no loss of generality to assume that we need to translate  $\alpha$  and  $\beta$  for  $B$  to propagate in the same direction as its interaction; hence,

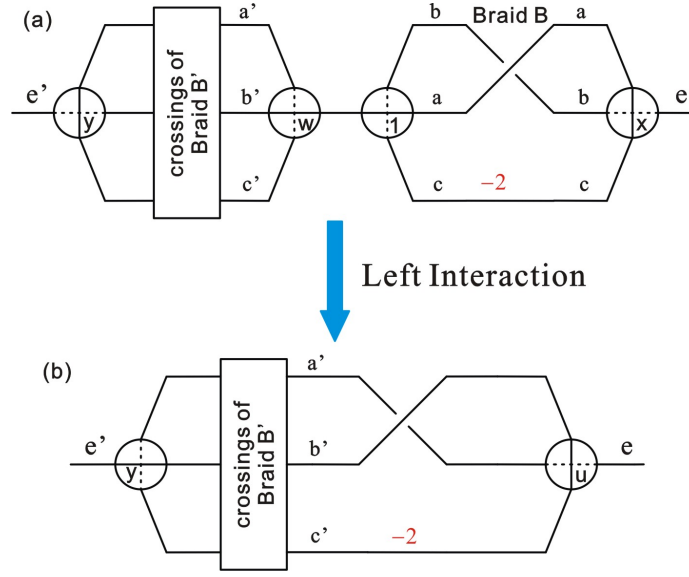


Figure 26: The braid in Fig. 24 can also interact from the left.

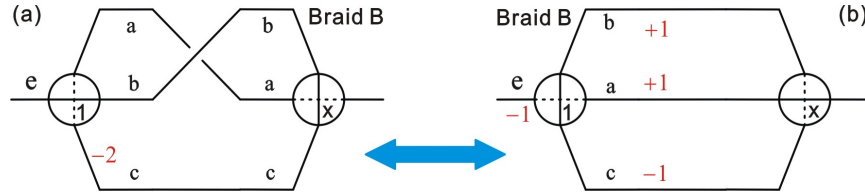


Figure 27: The braid in 24 is equivalent to a trivial braid with twists.

after the translation we must demand that  $\alpha$ ,  $\beta$ , and node 1 can be rearranged in a proper configuration for a  $3 \rightarrow 2$  move. So the question is, if  $\alpha$ ,  $\beta$ ,  $\gamma$  and 1 can be configured for a  $4 \rightarrow 1$  move, can we also configure  $\alpha$ ,  $\beta$ , and 1 for a  $3 \rightarrow 2$  move?

Let us consider active right-interaction. In the proper configuration for a  $4 \rightarrow 1$  move, we rename  $\alpha$ ,  $\beta$ , and  $\gamma$  by the permutation of 2, 3 and 4, since we don't know the relative positions of  $\alpha$ ,  $\beta$ , and  $\gamma$  after their translation over the crossings of an arbitrary braid  $B$ ; the situation is shown in Fig. 29(a). We assumed the propagation of braid  $B$  requires translating  $\alpha$  and  $\beta$ ; however, we don't know really know the renaming of  $\alpha$  and  $\beta$  after their translation within an arbitrary braid  $B$ ; they can be 2 and 3, or 2 and 4, or 3 and 4. Therefore, to prove that right-interaction implies right-propagation, it suffices to show that one can always re-arrange nodes 1, 2 and 3, or 1, 2, and 4, or 1, 3, and 4 in a proper configuration for a  $3 \rightarrow 2$  move if 1, 2, 3 and 4 can be configured as in Fig. 29(a).

Fig. 29 clearly illustrates the procedure of re-arranging nodes 1, 3, and 4 in a proper configuration for a  $3 \rightarrow 2$  move (compare the green loop in (c) with Fig. 12(b)), from the

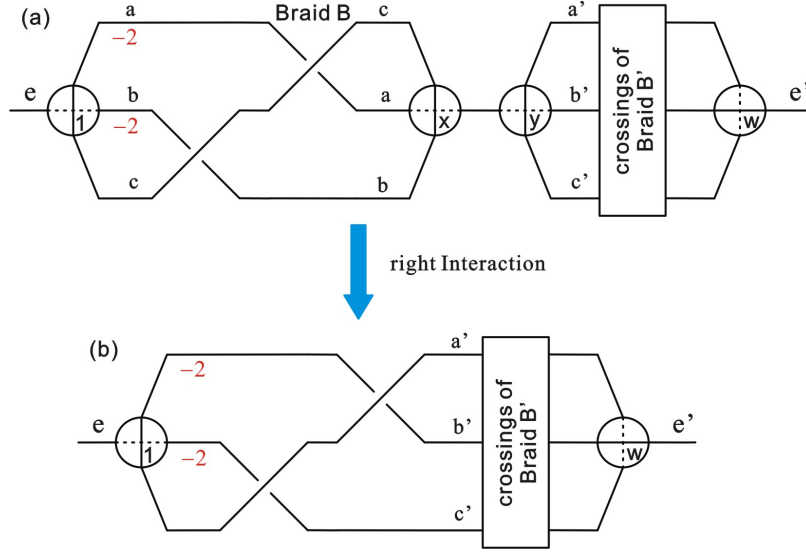


Figure 28: A second example of a right braid interaction.

proper configuration of 1, 2, 3, and 4 for a  $4 \rightarrow 1$  move. Interestingly and fortunately, all the equivalence moves taking 1, 3, and 4 in 29(a) to them in (c) do not result in any twist along the green loop, which satisfies Condition 2; this is a subtlety of the proof. As a consequence of symmetry, nodes 1, 2, and 4 in Fig. 29(a) can also be configured properly for a  $3 \rightarrow 2$  move. The case of re-arranging nodes 1, 2, and 3 in Fig. 29(a) in a proper configuration for a  $3 \rightarrow 2$  move is depicted in Fig. 30.

The proof in the case of an active left-interaction follows immediately by similarity and symmetry. Therefore, the theorem is proved.

As a closing remark, the validity of the theorem can also be seen if one looks at the local dual picture of a  $4 \rightarrow 1$  move, in which four tetrahedra stick together forming a new tetrahedron; any three of them can form two tetrahedra by a  $3 \rightarrow 2$  Pachner move. The above proof simply interpret this topological picture in a clear way with our notation of the embedded spinnets. In fact, the examples we have found of actively interacting braids are all reducible to an unbraid with twists. This is consistent with these general results.  $\square$

## 7 Conclusions

We have considered here the interaction and propagation of locally topologically stable braids in four valent graphs of the kind that occur in loop quantum gravity and spin foam models. The dynamics is restricted to those coming from the dual Pachner moves, which includes the widely studied spin foam models. The graphs representing the states are embedded in a three manifold up to diffeomorphisms. We considered both the framed

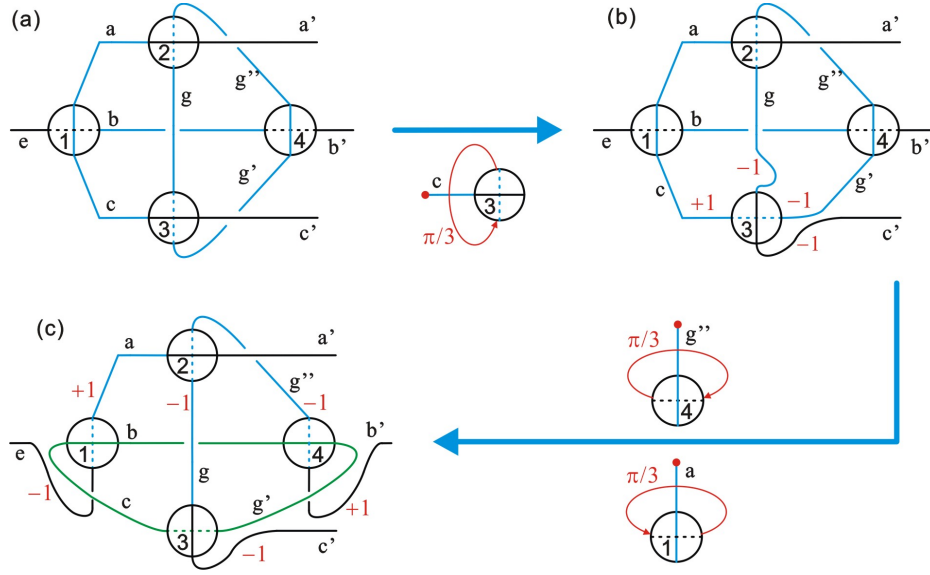


Figure 29: This figure shows the full procedure of re-arranging nodes 1, 3, and 4 in (a) in a proper configuration for a  $3 \rightarrow 2$  move, which is illustrated in (c). Note that the green loop in (c) is twist free after rotating nodes 1 and 4 from (b).

and unframed cases. We also neglected the labels or colours on the spin networks as our results do not depend on them, nor do they depend on the precise amplitudes of the dual Pachner moves, so long as they are non-vanishing.

We studied braids made up of two four valent nodes sharing three edges and found there are three classes of graphs.

- Actively interacting braids, which also propagate. All the examples found so far are completely reducible to an unbraid with twisted edges. This means that they are characterized by three integers which give the twists on the three edges.
- Braids which propagate but are not actively interacting. The possibilities for these are limited by general results we found.
- Braids, which are neither propagating or interacting.

It is very interesting to note that the braids required in the three-valent case to realize Bilson-Thompson's preon mode[4] also are classified by three integers representing twists on an unbraid[8]. This suggests that it may be possible to incorporate a preon model with interactions within the dynamics of four-valent braids studied here.

There are other interesting research lines in this direction. For example, in usual settings of spinfoam models, tensor models or group field theories, graphs are unembedded and labeled by elements of the appropriate permutation groups, and are then called fat



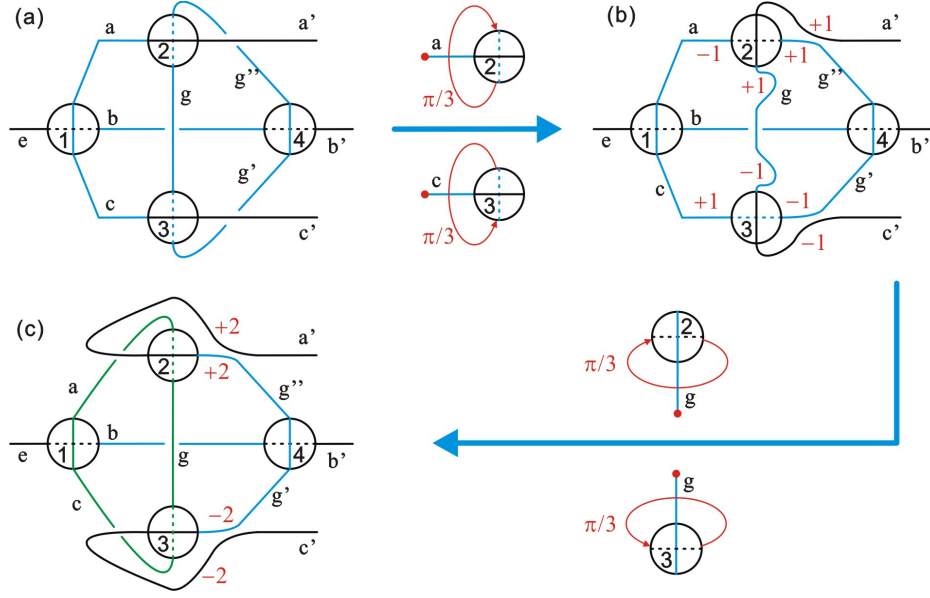


Figure 30: This figure shows the full procedure of re-arranging nodes 1, 2, and 3 in (a) in a proper configuration for a  $3 \rightarrow 2$  move, which is illustrated in (c). Note that the green loop in (c) is twist free after rotating nodes 2 and 3 from (b).

graphs. There is an explicit criterion to decide whether the simplicial complex associated to a given fat graph as a Feynman diagram of a suitable field theory is a manifold or not[12]. It would be very interesting to clarify the relationship between the unembedded fat graphs and our embedded (framed) graphs and to see if our results also apply in the usual spinfoam or group field theory settings. Recently, Premont-Schwarz has also obtained related results in the unembedded case[13].

## Acknowledgements

We thank Fotini Markopoulou for initial collaboration on this project, including the suggestion to examine braids in four valent graphs with a restricted set of dual Pachner moves. We are also grateful for discussions and comments with Sundance Bilson-Thompson, Jonathan Hackett, Louis Kauffman and Isabeau Premont-Schwarz. Research at Perimeter Institute is supported in part by the Government of Canada through NSERC and by the Province of Ontario through MEDT.

## References

- [1] F. Markopoulou, *Towards gravity from the quantum*, arXiv:hep-th/0604120.

- [2] D. W. Kribs, F. Markopoulou, *Geometry from quantum particles*, gr-qc/0510052. F. Markopoulou and D. Poulin, *Noiseless subsystems and the low energy limit of spin foam models*, unpublished.
- [3] S. Bilson-Thompson, F. Markopoulou, L. Smolin, *Quantum gravity and the standard model*, arXiv:hep-th/0603022
- [4] S. O. Bilson-Thompson, *A topological model of composite preons*, hep-ph/0503213.
- [5] S. Major and L. Smolin, *Quantum deformation of quantum gravity*, Nucl. Phys. B473, 267(1996), gr-qc/9512020; R. Borissov, S. Major and L. Smolin, *The geometry of quantum spin networks*, Class. and Quant. Grav.12, 3183(1996), gr-qc/9512043; L. Smolin, *Quantum gravity with a positive cosmological constant*, hep-th/0209079.
- [6] F. Markopoulou, *Dual formulation of spin network evolution* gr-qc/9704013; F. Markopoulou, Lee Smolin, Phys.Rev. D58 (1998) 084032, gr-qc/9712067.
- [7] J. Hackett, *Locality and Translations in Braided Ribbon Networks*, hep-th/0702198.
- [8] S. Bilson-Thompson, J. Hackett, L. Kauffman, in preparation.
- [9] F. Markopoulou, personal communication.
- [10] Carlo Rovelli, *Loop Quantum Gravity*, Living Rev.Rel. 1 (1998) 1, gr-qc/9710008; *Quantum Gravity*, Cambridge University Press, 2004.
- [11] Y. Wan, *On Braid Excitations in Quantum Gravity*, arXiv:0710.1312.
- [12] R. De Pietri, C. Petronio, *Feynman Diagrams of Generalized Matrix Models and the associated Manifolds in Dimension 4*, J. Math. Phys. 41, (2000) 6671, gr-qc/0004045.
- [13] I. Premont-Schwarz, in preparation.